Check for updates

View Article Online
View Journal

Sustainable Energy & Fuels

Interdisciplinary research for the development of sustainable energy technologies

Accepted Manuscript

This article can be cited before page numbers have been issued, to do this please use: M. Steponaitis, M. La-Placa, I. C. KAYA, G. Bubniene, V. Jankauskas, M. Daskeviciene, M. Sessolo, T. Malinauskas, H. J. Bolink and V. Getautis, *Sustainable Energy Fuels*, 2020, DOI: 10.1039/D0SE00728E.

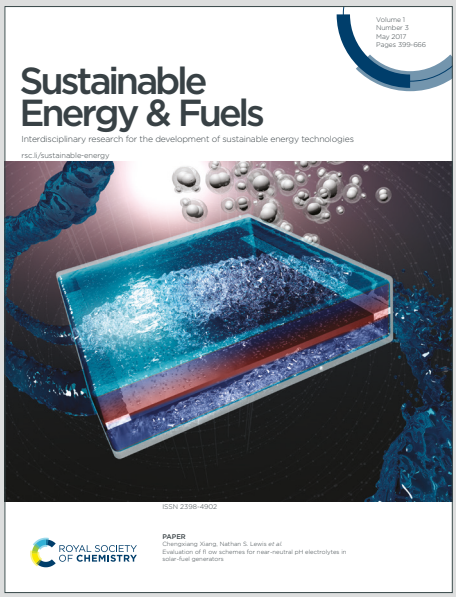

This is an Accepted Manuscript, which has been through the Royal Society of Chemistry peer review process and has been accepted for publication.

Accepted Manuscripts are published online shortly after acceptance, before technical editing, formatting and proof reading. Using this free service, authors can make their results available to the community, in citable form, before we publish the edited article. We will replace this Accepted Manuscript with the edited and formatted Advance Article as soon as it is available.

You can find more information about Accepted Manuscripts in the Information for Authors.

Please note that technical editing may introduce minor changes to the text and/or graphics, which may alter content. The journal's standard Terms & Conditions and the Ethical guidelines still apply. In no event shall the Royal Society of Chemistry be held responsible for any errors or omissions in this Accepted Manuscript or any consequences arising from the use of any information it contains.

Please do not adjust margins

View Article Online
DOI: 10.1039/D0SE00728E

ARTICLE

Enamine-based hole transporting materials for vacuum-deposited perovskite solar cells

Received 00th January 20xx,
Accepted 00th January 20xx

DOI: 10.1039/x0xx00000x

Matas Steponaitis[a], Maria-Grazia La-Placa[b], İsmail Cihan Kaya[b], Giedre Bubniene[a], Vygintas Jankauskas[c], Maryte Daskeviciene[a], Michele Sessolo[b]†, Tadas Malinauskas[a]†, Henk J. Bolink[b] and Vytautas Getautis[a].

In a short period of time rapid development of perovskite solar cells attracted a lot of attention in the science community with record for power conversion efficiency being broken every year. Despite the fast progress in power conversion efficiency there are still many issues that need to be solved before starting large scale commercial application, among others, the difficult and costly synthesis and usage of toxic solvents for the deposition of hole transport materials (HTMs). We report new enamine-based charge transport materials obtained via simple one step synthesis procedure, from commercially available precursors and without the use of expensive organometallic catalysts. The developed materials demonstrated rapid loss of mass during thermogravimetry analysis suggesting that they could be processed not only using solution processing, but also via vacuum deposition technique. Furthermore, all HTMs demonstrated high charge carrier mobility with H2 possessing the highest mobility of $2.5 \cdot 10^{-2}$ $cm^2V^{-1}s^{-1}$ at strong electric fields. The investigated materials were employed in vacuum-deposited p-i-n perovskite solar cells and champion devices with enamine H2 demonstrated PCE of 18.4%.

Introduction

The growth of human population and the technological progress in the last hundred years has dramatically increased the global energy consumption [1]. With limited fossil fuel resources and the overall rise in pollution, renewable energy sources have become an attractive alternative. One of the most promising alternatives are photovoltaic devices. In recent years the field of perovskite solar cells (PSCs) attracted large attention mostly due to the easily tuneable band gap of the perovskite [2], relatively simple device fabrication [3;4] and the continuously increasing power conversion efficiency (PCE) with current record being 25.2 % [5]. PSCs can be fabricated in two configurations, n-i-p or p-i-n, identified depending on the type of charge selective layer which is deposited onto the front transparent contact (in n-i-p and p-i-n, n- and p-type layers are used as the front contact, respectively). n-i-p devices usually use compact or mesoporous TiO_2 or SnO_2 [6;7;8;9] as the electron transport layer (ETL), deposited on transparent conductive oxide (TCO) substrates. On top of the ETL, the perovskite, a hole transport layer (HTL) and a metal cathode are subsequently deposited [10]. The main architectural differences between p-i-n and n-i-p PSCs are the materials used as ETL and HTL as well as the order in which they are deposited [11].

p-i-n PSCs have several advantages compared to n-i-p devices: i) the high temperature needed for TiO_2 annealing is avoided; ii) low-cost copper can be used as a cathode instead of silver or gold [12]; iii) p-i-n architecture enables higher PCE potential in tandem cells due to lower parasitic absorption in the front contact [13, 14].

Currently some of the most widely used hole transport materials (HTMs) for p-i-n PSCs are (semi)conducting polymers such as poly-TPDs [15;16], PTAA [17;18], PEDOT:PSS [15;19] and metal oxides as CuOx [20;21], NiOx [20;22]. The aforementioned organic compounds are often deposited using spin-coating technique, which is cost wise very inefficient and not suitable for large-scale fabrication. As an alternative, perovskite solar cells can be fabricated by vacuum deposition, which is widely used in the industry and hence suitable to scale up the device preparation. Moreover, it avoids use of toxic solvents which are usually employed in the fabrication of PSCs [23] and allows to more accurately control the processing of multilayer stacks [24]. However, its application is limited to relatively small molecules as they need to be sublimed [25]. Herein new enamine-based HTMs were synthesized in a simple single step reaction from commercially available materials without the use of expensive transition metal catalysts. The compounds were synthesized in order to have a relatively large ionization energy, which should match the perovskite absorber

[a] Department of Organic Chemistry, Kaunas University of Technology, Radvilenu pl. 19, LT-50254, Kaunas, Lithuania.
[b] Instituto de Ciencia Molecular, Universidad de Valencia, C/Catedrático J. Beltrán 2, 46980 Paterna, Spain.
[c] Institute of Chemical Physics, Vilnius University Sauletekio al.3, Vilnius LT-10257, Lithuania
† Corresponding authors: michele.sessolo@uv.es, tadas.malinauskas@ktu.lt
Electronic Supplementary Information (ESI) available: [details of any supplementary information available should be included here]. See DOI: 10.1039/x0xx00000x

Published on 27 July 2020. Downloaded by Kaunas University of Technology on 7/29/2020 10:50:42 AM.

Sustainable Energy & Fuels Accepted Manuscript

Please do not adjust margins

View Article Online
DOI: 10.1039/D0SE00728E

Published on 27 July 2020. Downloaded by Kaunas University of Technology on 7/29/2020 10:50:42 AM.

to ensure efficient hole extraction. The HTMs exhibited high thermal stability and large carrier drift mobility, reaching $2.5 \cdot 10^{-2}$ $cm^2V^{-1}s^{-1}$ (H2) at strong electric fields. All materials were tested in fully vacuum-processed p-i-n PSCs, showing performance comparable to state-of-the-art evaporated devices.

Results and discussion

Synthesis

Synthesis of enamines H1, H2, H3 and H4 was conducted using single-step acid catalysed condensation reaction. Carbazole was condensed with diphenylacetaldehyde using camphor-10-sulfonic acid (β) (CSA) as a catalyst in toluene to give enamine H1 (Scheme 1). The same reaction conditions were applied in case of m-tolidine to obtain H3 as desired product.

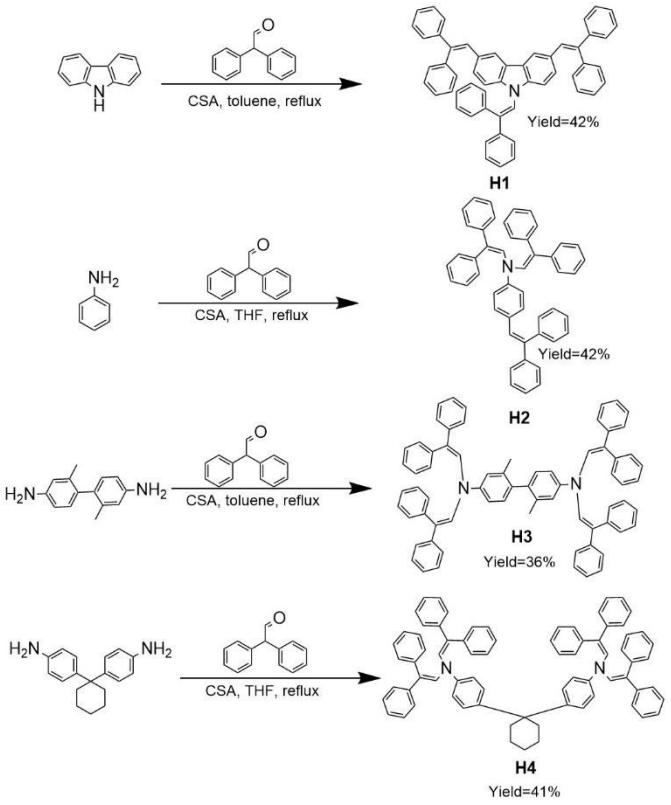

Scheme 1. Synthesis of enamine H1, H2, H3 and H4.

Enamines H2 and H4 were synthesized in the same type of one step condensation reaction of aniline or 1,1-bis(4-aminophenyl)cyclohexane with diphenylacetaldehyde utilizing CSA, although in this case THF was used as a solvent instead of toluene (Scheme 1). The mechanisms for the above mentioned reactions were reported in earlier publications [26;27].

After performing extraction H1 and H2 are purified by column chromatography, while H4 follows the same pattern except extraction is replaced with precipitation by pouring the cooled reaction mixture into methanol. HTM H3 requires the simplest purification: the cooled reaction mixture is poured into ethyl acetate and formed crystals are filtered and washed with methanol and ethyl acetate.

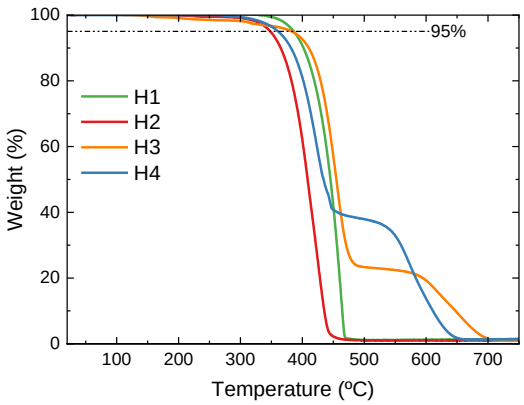

Figure 1. TGA heating curves of H1, H2, H3 and H4.

Thermal properties

Thermal stability of the materials was measured using thermogravimetric analysis (TGA) and the results can be seen in Figure 1 and Table 1. All tested HTMs showed 5% weight loss at temperatures higher than 300 °C, proving that they are sufficiently thermally stable for application in PSCs. Furthermore, the rapid weight loss seen in Figure 1 indicates that investigated materials can sublime and could be vacuum deposited.

Analysis of differential scanning calorimetry (DSC) data showed that materials H1, H2 and H4 have relatively high glass transition temperatures (T_g), above 100°C (Table 1). This might be beneficial for the stability of PSCs under working conditions, when the temperature can exceed 65 °C [28]. The aforementioned compounds can be both amorphous and crystalline with melting temperatures (T_m) higher than 200°C for H1, H2. H4 demonstrates crystallization at 202°C and subsequent melting of the crystals at 315°C during first heating.

Table 1. Thermal characteristics of the HTMs.

Compound	T_g [a], °C	T_m [b], °C	T_{dec} [c], °C
H1	111	215	386
H2	110	235	348
H3	-	339	361
H4	156	315	383

a) Determined by DSC: scan rate = 10 °C min^{-1}, N_2 atmosphere; second run; b) Determined by DSC: scan rate = 10 °C min^{-1}, N_2 atmosphere; first run; c) Onset of decomposition determined by TGA: heating rate = 10 °C min^{-1}, N_2 atmosphere.

Sustainable Energy & Fuels Accepted Manuscript

This journal is © The Royal Society of Chemistry 20xx

Please do not adjust margins

View Article Online
DOI: 10.1039/D0SE00388E

Published on 27 July 2020. Downloaded by Kaunas University of Technology on 7/29/2020 10:50:42 AM.

Interestingly m-tolidine derivative H3, is a crystalline material with T_m observed at 339°C. The lack of T_g could be explained by the spatial configuration of diphenylacetaldehyde substituents and the two methyl groups in the meta- position of m-tolidine fragment. Introduction of the structural symmetry in H3, compared with H2, leads to higher melting temperature and increased tendency to crystallize. It is verified by absence of glass transition during first and second heating runs, presence of exothermic crystallization peak at 239°C during rapid cooling and endothermic melting peak at 330°C during second heating run in DSC curves for H3 (Figure S1).

Optical and Photoelectrical properties

Light absorption and emission characteristics of HTMs H1, H2, H3 and H4 were measured in toluene solutions and on a glass substrate. Compounds H1 and H2 contain three phenylethenyl substituents and differ only by the central core (carbazole in H1 and aniline in H2), however that is enough to influence optical properties. Differences in absorption spectra between these two materials are noticeable both in solution and on a glass substrate.

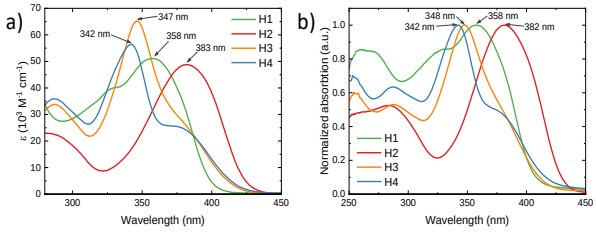

Figure 2. a) UV-vis absorption spectra of H1, H2, H3, H4 in toluene and b) thin-films on glass.

Observed redshift (~25 nm) in the UV-vis absorption spectra for the aniline derivative H2, compared with carbazole HTM H1 (Figure 2a; Figure 2b) could be explained by the structural difference of the central core of H1 and H2 [29;30]. The same tendencies can be seen for the emission spectra: after excitation, H1 emits shorter wavelength light than H2 (Figure S2; Figure S3).

Table 2. Absorption and photoluminescence (PL) data

Compound	λ_{max}^{abs}, nm (a)	λ_{max}^{abs}, nm (b)	PL, nm (c)	PL, nm (d)
H1	358	358	458	479
H2	383	382	470	495
H3	347	348	490	499
H4	342	342	496	494

a) Absorption maxima in toluene; b) Absorption maxima on glass substrate; c) Fluorescence maxima in toluene; d) Fluorescence maxima on glass substrate

H3 and H4 are structurally similar molecules both containing four phenylethenyl substituents connected via two aniline derivatives with the biggest difference being interruption of the conjugation in H4 by a cyclohexane fragment. The aforementioned separation has little effect on the absorption and emission properties when comparing H3 with H4 (Table 2). The most notable difference can be seen in the intensity of absorption in the solution, H3 demonstrates more intense absorption than H4 (Figure 2a) [29]. This could be explained by the slightly lower π-conjugation of H4 due to somewhat larger steric hindrances in the molecule compared to H3.

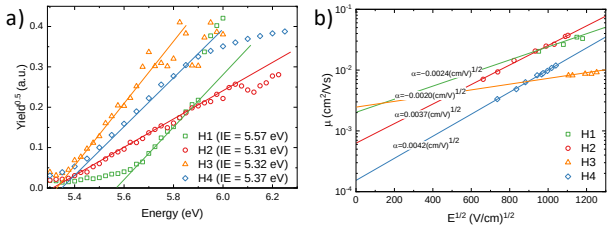

Figure 3. a) I_p measurements of compounds H1, H2, H3 and H4. b) Charge carrier mobility of the tested materials.

Ionization energy (I_p) of the investigated p-type semiconductors were measured by photoemission spectroscopy in air (Figure 3a). Materials H2, H3 and H4 have I_p values in the 5.30 – 5.40 eV range, while H1 has higher I_p of 5.57 eV (Table 3). The large difference of I_p between H2–H4 and H1 is most likely due to the fact that H1 contains carbazole fragment, while other tested HTMs can be viewed as aniline derivatives [29;30].

Table 3. Photophysical properties of the synthesized materials.

Compound	I_p, eV (a)	μ_0, $cm^2V^{-1}s^{-1}$ (b)	μ, $cm^2V^{-1}s^{-1}$ (c)	$\alpha^{(d)}$
H1	5.57	$2.1\cdot10^{-3}$	$2.3\cdot10^{-2}$	0.0024
H2	5.31	$6\cdot10^{-4}$	$2.5\cdot10^{-2}$	0.0037
H3	5.32	$2.4\cdot10^{-3}$	$7\cdot10^{-3}$	0.0020
H4	5.37	$1.5\cdot10^{-4}$	$1\cdot10^{-2}$	0.0042

a) Ionization energy was measured by photoemission spectroscopy in air from films; b) Hole mobility value at zero field strength; c) Hole mobility value at the electric field strength of $6.4\cdot10^5$ Vcm^{-1}; d) Poole–Frenkel parameter.

The charge carrier mobility of HTMs was measured from films by xerographic time-of-flight (XTOF) method (Figure 3b). All materials displayed excellent charge transport properties, well above $1\cdot10^{-3}$ $cm^2V^{-1}s^{-1}$ (Table 3), rivalling some of the best organic HTMs used in PSCs [31]. The good drift carrier mobility of tested materials could be explained by more efficient charge hopping due to more favourable arrangement of molecules [32].

Sustainable Energy & Fuels Accepted Manuscript

View Article Online
DOI: 10.1039/D0SE00728E

Published on 27 July 2020. Downloaded by Kaunas University of Technology on 7/29/2020 10:50:42 AM.

Sustainable Energy & Fuels Accepted Manuscript

Device performance

Perovskite solar cells with the p-i-n configuration (Figure 4a) were prepared by vacuum deposition following previously published protocols (details in the Supplementary information) [33]. Briefly, glass slide with indium tin oxide (ITO) patterned electrodes were coated with MoO_3 (5 nm), the hole transport layer (HTL, 10 nm), a 500 nm thick methylammonium lead iodide (MAPI) absorber, C_{60} (25 nm), bathocuproine (BCP, 8 nm) and silver (100 nm). MoO_3 was used to increase the work function at the front electrode and enhance charge extraction from the HTL to the ITO [34]. All four HTLs were tested in devices, and at least 8 pixels were measured for each material.

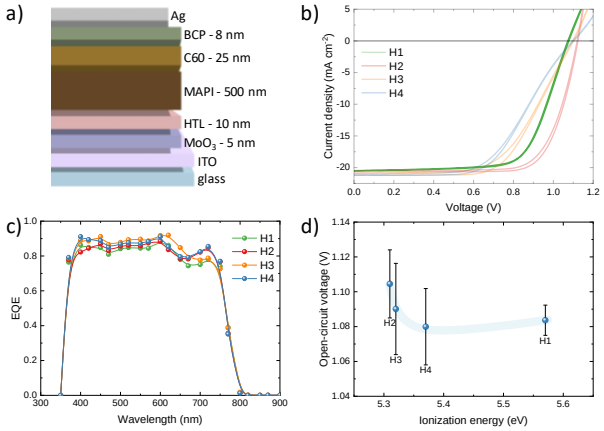

Figure 4. a) Solar cell layout with materials and corresponding film thickness. b) J-V curves under simulated solar illumination and c) EQE spectra for solar cells employing the different HTLs. d) Trend of the solar cells Voc as a function of the ionization energy of the HTL.

The solar cells were characterized by measuring the current density as a function of the applied voltage (J-V curves, Figure 4b), under simulated solar illumination, in forward (from short to open circuit) and reverse (from open to short circuit) bias. J-V curves showed only small hysteresis between the forward and reverse bias, which might indicate the presence of interfacial recombination [35]. The characteristic photovoltaic parameters (extracted from the forward J-V scans) as a function of the HTL used are reported in Table 4. The short-circuit current J_{sc} was found to vary only in the 20.5-21 mA cm^{-2} range among the series of devices with different HTLs, due to their high transparency in the visible part of the electromagnetic spectrum. This is confirmed by the spectral response of the solar cells (external quantum efficiency, Figure 4c), which is similar for the entire series, fluctuating between EQE values of 0.8 and 0.9. More striking are the differences in fill factor (*FF*), which reflects the efficiency of the charge transport and extraction processes. Solar cells with H3 and H4 showed a pronounced kink in the J-V curve under illumination, which result in average *FF* limited to 56.8% and 53.8%, respectively.

Table 4. Photovoltaic parameter extracted from p-i-n solar cells employing different HTLs (10 nm thick).

HTL		J_{sc}, mA/cm²	V_{oc}, mV	*FF*, %	PCE, %
H1	*average*	20.5	1084	67.6	15.0
	best	20.5	1078	69.3	15.3
H2	*average*	20.5	1105	71.8	16.3
	best	20.8	1130	74.9	17.6
H3	*average*	20.8	1090	56.8	12.9
	best	21.2	1101	61.1	14.3
H4	*average*	20.8	1080	53.8	12.1
	best	21.1	1110	56.3	13.2

The *FF* was slightly higher for cells with H1, reaching 67.6% on average, and the maximum value was obtained when employing H2 as the HTL, with an average *FF* of 71.8% and as high as 74.9% for the best pixels. The origin of this trend is not clear, as we did not observe a correlation with the charge carrier drift mobility (Table 3) nor with the ionization energy of the materials. A more apparent trend was observed for the open-circuit voltage (V_{oc}), which was found to scale inversely with the ionization energy of the HTLs (Figure 4d). This observation is likely related with the alignment of the highest occupied molecular orbital (HOMO) of the HTL (estimated by the ionization energy) and the maximum of the valence band (VBM) of the perovskite. While the V_{oc} of perovskite solar cells is rather insensitive to the HOMO of the HTLs [36;37], there is a consensus towards the need to minimize the energy barriers for charge extraction to maximize voltage and FF [38]. In this case, the higher photovoltage (1105 mV on average, with highest at 1130 mV) measured for H2 agrees with recent measurements of the VBM for MAPI, estimated at 5.2 eV from the vacuum level [39]. On the other extreme, solar cells employing H1 as the transport material (ionization energy > 5.5 eV) delivered V_{oc} of approximately 1080 mV. The overall efficiency of the devices with H2 was found to be the highest in the series, with PCE of 16.3% on average and the best pixel at 17.6%. In view of the promising performance of H2 in our vacuum deposited perovskite solar cells, we have fabricated additional cells with

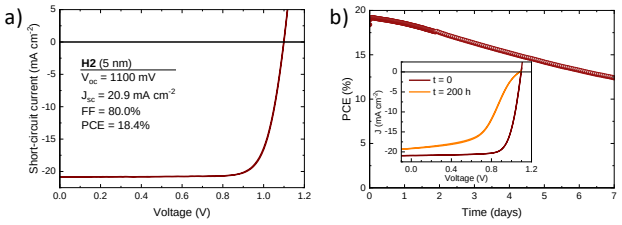

Figure 5. a) J-V curve of a representative solar cell using a 5 nm thick H2 film as the hole transport layer. b) Evolution of the efficiency measured under continuous illumination with maximum power point tracking over a week. The inset shows the J-V curves of the device before and after 200 hours of continuous illumination.

This journal is © The Royal Society of Chemistry 20xx

Please do not adjust margins

Published on 27 July 2020. Downloaded by Kaunas University of Technology on 7/29/2020 10:50:42 AM.

thinner HTL (5 nm instead of 10 nm), as this might alleviate transport losses within the organic semiconductor and increase the built-in potential [36].

Solar cells with 5 nm thick H2 show a very good rectification, fully suppressed hysteresis and *FF* as high as 80%, maintaining essentially unvaried the other photovoltaic parameters (Figure 5a). The improvement in *FF* led to PCE as high as 18.4%, which is close to the highest reported for vacuum-processed p-i-n devices [33;40] (about 19%). We further tested the solar cells over time, under continuous simulated solar illumination. The devices were encapsulated with UV-curable resin and a glass slide and kept at 25 °C under a nitrogen flow (max relative humidity 10%), to minimize the effect of the environment. The maximum power point was continuously tracked and the evolution of the PCE over time is depicted in Figure 3b. The solar cell showed an initial rise in efficiency (to about 19%) followed by a slow but continuous decay for the 7 days of characterization. After one week of continuous operation, the device with H2 contact delivered a PCE of 12.5%, which was found to be mainly determined by the decrease in FF (see inset in Figure 5b) and to a less extent by a lower current density. While the latter points towards a degradation of the MAPI perovskite film, we cannot exclude other degradation pathways related with interfacial effects at the front contact.

Cost estimation

To evaluate the cost-effectiveness of the best performing material H2, we calculated the estimated cost of its synthesis based on the procedure established by Osedach et al. (Table S1) [41]. Moreover, the cost of spiro-TTB, an often used p-type semiconductor in vacuum deposited PSCs [37], was calculated based on articles by M. L. Petrus et al. and Yin et al (Table S2) [42;43]. It was estimated that the cost of our HTM is about 19$ per gram which is less than 1/3 of spiro-TTB (about 67$ per gram). Furthermore, synthesis of H2 is done in a single step reaction and does not require expensive palladium catalysis, avoiding traces of organic impurities and catalyst residue that could act as photoquenchers or charge traps [44;45].

Conclusions

We have synthesized new enamine-based compounds using single step reaction without the use of expensive transition metal catalysts. Despite structural differences all HTMs displayed excellent charge transport properties with H2 reaching hole mobility $2.5 \cdot 10^{-2}$ $cm^2V^{-1}s^{-1}$ at strong electric fields. Furthermore, all materials exhibited relatively high T_g and T_m, great thermal stability and rapid weight loss during TGA, which allowed processing of these HTMs in p-i-n architecture PSCs via vacuum-deposition. H2 demonstrated the best PCE with the champion cell reaching 18.4% efficiency. Above-mentioned results and properties designate these compounds as attractive materials for large scale PSC applications.

Conflicts of interest

View Article Online
DOI: 10.1039/D0SE00728E

There are no conflicts to declare.

Acknowledgements

The research leading to these results had received funding from the European Union's Horizon 2020 research and innovation program under grant agreement No. 763977 of the PerTPV project. The authors acknowledge funding from Research Council of Lithuania (grant No. MIP-17-70) and E. Kamarauskas for measurements of ionization potential. Further acknowledgments to Spanish Ministry of Science, Innovation and Universities, MAT2017-88821-R, RTI2018-095362-A-I00, PCI2019-111829-2 and EQC2018-004888-P, and the Comunitat Valenciana, IDIFEDER/2018/061. M.S. acknowledges the Spanish Ministry for his RyC contract.

References

1 H. Ritchie and M. Roser (2019) - "Energy Production & Changing Energy Sources". Published online at OurWorldInData.org. Retrieved from: 'https://ourworldindata.org/energy-production-and-changing-energy-sources' [Online Resource].
2 M. Saliba, J. P. Correa-Baena, M. Graetzel, A. Hagfeldt, A. Abate, Angew. Chem. Int. Ed., 2018, **57**, 2554.
3 Z. Shi, A. H. Jayatissa, Materials, 2018, **11**, 729
4 Z. Li, T. R. Klein, D. H. Kim, M. Yang, J. J. Berry, M. F. A. M. van Hest, K. Zhu, Nat. Rev. Mater., 2018, **3**, 18017.
5 M. A. Green, E. D. Dunlop, J. Hohl-Ebinger, M. Yoshita, N. Kopidakis, A. W.Y. Ho-Baillie, Prog Photovolt: Res Appl., 2020, **28**, 3.
6 Q. Jiang, L. Zhang, H. Wang, X. Yang, J. Meng, H. Liu, Z. Yin, J. Wu, X. Zhang, J. You, Nat. Energy, 2016, **2**, 16177.
7 E. H. Jung, N. J. Jeon, E. Y. Park, C. S. Moon, T. J. Shin, T. Y. Yang, J. H. Noh, J. Seo, Nature, 2019, **567**, 511.
8 M. M. Lee, J. Teuscher, T. Miyasaka, T. N. Murakami, H. J. Snaith, Science, 2012, **338**, 643.
9 H. S. Kim, C. R. Lee, J. H. Im, K. B. Lee, T. Moehl, A. Marchioro, S. J. Moon, R. Humphry-Baker, J. H. Yum, J. E. Moser, M. Gratzel, N. G. Park, Sci Rep., 2012, **2**, 591.
10 H. Li, K. Fu, A. Hagfeldt, M. Gratzel, S. G. Mhaisalkar, A. C. Grimsdale, Angew. Chem. Int. Ed., 2014, **53**, 4085.
11 M. Saliba, J. P Correa-Baena, C. H. Wolff, M. Stolterfoht, N. Phung, S. Albrecht, D. Neher, A. Abate, Chem. Mater., 2018, **30**, 4193.
12 J. Zhao, X. Zheng, Y. Deng, T. Li, Y. Shao, A. Gruverman, J. Shield, J. Huang, Energy Environ. Sci., 2016, **9**, 3650.
13 K. Jäger, L. Korte, B. Rech, S. Albrecht, Opt. Express, 2017, **25**, A473.
14 K. A. Bush, A. F. Palmstrom, Z. J. Yu, M. Boccard, R. Cheacharoen, J. P. Mailoa, D. P. McMeekin, R. L. Z. Hoye, C. D. Bailie, T. Leijtens, I. M. Peters, M. C. Minichetti, N. Rolston, R. Prasanna, S. Sofia, D. Harwood, W. Ma, F. Moghadam, H. J. Snaith, T. Buonassisi, Z. C. Holman, S. F. Bent, M. D. McGehee, Nat. Energy, 2017, **2**, 17009.
15 D. Zhao, M. Sexton, H. Y. Park, G. Baure, J. C. Nino, F. So, Adv. Energy Mater., 2014, **5**, 1401855.
16 J. T.-W. Wang, Z. Wang, S. Pathak, W. Zhang, D. W. deQuilettes, F. Wisnivesky-Rocca-Rivarola, J. Huang, P. K. Nayak, J. B. Patel, H. A. Mohd Yusof, Y. Vaynzof, R. Zhu, I. Ramirez, J. Zhang, C. Ducati, C. Grovenor, M. B. Johnston, D.

Sustainable Energy & Fuels Accepted Manuscript

S. Ginger, R. J. Nicholas, H. J. Snaith. Energy Environ. Sci., 2016, **9**, 2892.
17 J. H. Heo, H. J. Han, D. Kim, T. K. Ahn, S. H. Im, Energy Environ. Sci., 2015, **8**, 1602.
18 M. Stolterfoht, C. M. Wolff, Y. Amir, A. Paulke, L. Perdigón-Toro, P. Caprioglio, D. Neher, Energy Environ. Sci., 2017, **10**, 1530.
19 C. G. Wu, C.-H. Chiang, Z.-L. Tseng, M. K. Nazeeruddin, A. Hagfeldt, M. Grätzel, Energy Environ. Sci., 2015, **8**, 2725.
20 R. Rajeswari, M. Mrinalini, S. Prasanthkumar, L. Giribabu, Chem. Rec., 2017, **17**, 1.
21 C. Zuo, L. Ding, Small, 2015, **11**, 5528.
22 J. H. Kim, P.W. Liang, S.T. Williams, N. Cho, C. C. Chueh, M. S. Glaz, D. S. Ginger and A. K.Y. Jen, Adv. Mater., 2014, **27**, 695.
23 J. Ávila, C. Momblona, P.P. Boix, M. Sessolo, H. J. Bolink, Joule, 2017, **1**, 431.
24 J. Ávila, C. Momblona, P.P. Boix, M. Sessolo, M. Anaya, G. Lozano, K. Vandewal, H. Míguez, H. J. Bolink, Energy Environ. Sci., 2018, **11**, 3292.
25 C. Momblona, L. Gil-Escrig, E. Bandiello, E. M. Hutter, M. Sessolo, K. Lederer, J. Blochwitz-Nimoth, H. J. Bolink, Energy Environ. Sci. 2016, **9**, 3456.
26 G. Bubniene, T. Malinauskas, M. Daskeviciene, V. Jankauskas, V. Getautis, Tetrahedron, 2010, **66**, 3199.
27 Y J. Clayden, N. Greeves, S. Warren, Organic chemistry second edition, Oxford university press, 2012.
28 M. C. Alonso Garcia, J. L. Balenzategui, Renewable Energy, 2004, **29**, 1997.
29 D. Vaitukaityte, Z. Wang, T. Malinauskas, A. Magomedov, G. Bubniene, V. Jankauskas, V. Getautis, Henry J. Snaith, Adv. Mater. 2018, **30**, 1803735.
30 A. Sakalyte, J. Simokaitiene, A. Tomkeviciene, J. Keruckas, G. Buika, J. V. Grazulevicius, V. Jankauskas, C. P. Hsu, Chou-Hsun Yang, J. Phys. Chem. C., 2011, **115**, 4856.
31 W. Zhou, Z. Wen, P. Gao, Adv. Energy Mater., 2018, **8**, 1702512.
32 T. Malinauskas, M. Daskeviciene, G. Bubniene, I. Petrikyte, S. Raisys, K. Kazlauskas, V. Gaidelis, V. Jankauskas, R. Maldzius, S. Jursenas, V. Getautis, Chem. Eur. J., 2013, **19**, 15044.
33 A. Babaei, C. Dreessen, M. Sessolo, H. J. Bolink, RSC Adv., 2020, **10**, 6640.
34 A. Babaei, K. P. S. Zanoni, L. Gil-Escrig, D. Pérez-del-Rey, P. P. Boix, M. Sessolo, H. J. Bolink, Front. Chem., 2020, **7**, 936.
35 S. van Reenen, M. Kemerink, H. J. Snaith, J. Phys. Chem. Lett. 2015, **6**, 3808.
36 B. Danekamp, N. Droseros, D. Tsokkou, V. Brehm, P. P. Boix, M. Sessolo, N. Banerji, H. J. Bolink, J. Mater. Chem. C., 2019, **7**, 523.
37 R. A. Belisle, P. Jain, R. Prasanna, T. Leijtens, M. D. McGehee, ACS Energy Lett., 2016, **1**, 556.
38 C. M. Wolff, P. Caprioglio, M. Stolterfoht, Dieter Neher, Adv. Mater., 2019, **31**, 1902762.
39 J. Endres, D. A. Egger, M. Kulbak, R. A. Kerner, L. Zhao, S. H. Silver, G. Hodes, B. P. Rand, D. Cahen, L. Kronik, A. Kahn, J. Phys. Chem. Lett., 2016, **7**, 2722.
40 D. Perez-del-Rey, L. Gil-Escrig, K. P. S. Zanoni, C. Dreessen, M. Sessolo, P. P. Boix, H. J. Bolink, Chem. Mater., 2019, **31**, 6945.
41 T. P. Osedach, T. L. Andrew, V. Bulovic, Energy Environ. Sci., 2013, **6**, 711.
42 M. L. Petrus, T. Bein, T. J. Dingemans, P. Docampo, J. Mater. Chem. A, 2015, **3**, 12159.
43 C. Yin, J. Lu, Y. Xu, Y. Yun, K. Wang, J. Li, L. Jiang, J. Sun, A.D. Scully, F. Huang, J. Zhong, J. Wang, Y.-B. Cheng, T. Qin, W. Huang, Adv. Energy Mater. 2018, **8**, 1800538.
44 M. Degbia, M. Ben Manaa, B. Schmaltz, N. Berton, J. Boucle, R. Antony, F. Tran Van, Mater. Sci. Semicond. Process., 2016, **43**, 90.
45 O. Usluer, M. Cloutet, G. Hadziioannou, ACS Macro Lett., 2014, **3**, 1134.

View Article Online
DOI: 10.1039/D0SE00728E

Published on 27 July 2020. Downloaded by Kaunas University of Technology on 7/29/2020 10:50:42 AM.

Sustainable Energy & Fuels Accepted Manuscript

This journal is © The Royal Society of Chemistry 20xx

Please do not adjust margins

View Article Online
DOI: 10.1039/D0SE00728E

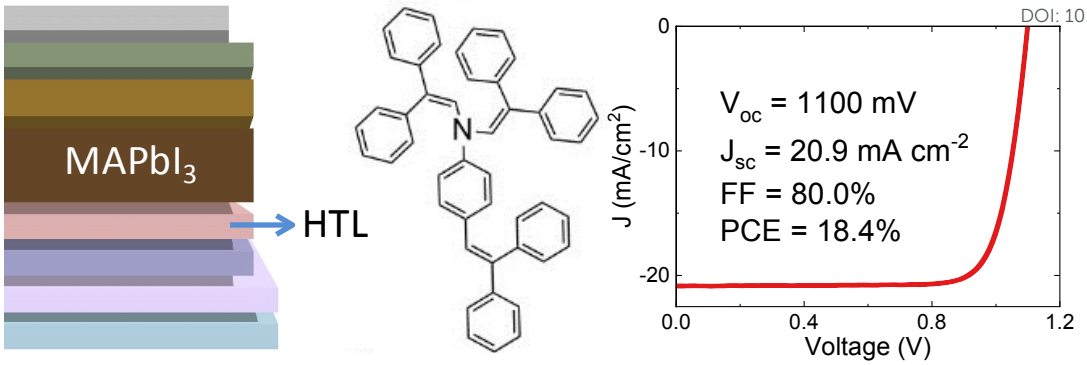

New sublimable enamine-based charge transport materials, obtained via simple one step synthesis, are used in efficient fully-vacuum deposited perovskite solar cells.

Published on 27 July 2020. Downloaded by Kaunas University of Technology on 7/29/2020 10:50:42 AM.

Sustainable Energy & Fuels Accepted Manuscript